



HAL
open science

Probing the theory of gravity with gravitational lensing of gravitational waves and galaxy surveys

Suvodip Mukherjee, Benjamin D. Wandelt, Joseph Silk

► To cite this version:

Suvodip Mukherjee, Benjamin D. Wandelt, Joseph Silk. Probing the theory of gravity with gravitational lensing of gravitational waves and galaxy surveys. *Monthly Notices of the Royal Astronomical Society*, 2020, 494 (2), pp.1956-1970. 10.1093/mnras/staa827 . hal-02302794

HAL Id: hal-02302794

<https://hal.science/hal-02302794>

Submitted on 28 May 2024

HAL is a multi-disciplinary open access archive for the deposit and dissemination of scientific research documents, whether they are published or not. The documents may come from teaching and research institutions in France or abroad, or from public or private research centers.

L'archive ouverte pluridisciplinaire **HAL**, est destinée au dépôt et à la diffusion de documents scientifiques de niveau recherche, publiés ou non, émanant des établissements d'enseignement et de recherche français ou étrangers, des laboratoires publics ou privés.

Probing the theory of gravity with gravitational lensing of gravitational waves and galaxy surveys

Suvodip Mukherjee,^{1,2★} Benjamin D. Wandelt^{1,2,3} and Joseph Silk^{1,2,4,5}

¹*Institut d’Astrophysique de Paris, 98 bis Boulevard Arago, F-75014 Paris, France*

²*Institut Lagrange de Paris, Sorbonne Universites, 98 bis Boulevard Arago, F-75014 Paris, France*

³*Center for Computational Astrophysics, Flatiron Institute, 162 5th Avenue, New York, NY 10010, USA*

⁴*Department of Physics & Astronomy, The Johns Hopkins University, 3400 N. Charles Street, Baltimore, MD 21218, USA*

⁵*Beecroft Institute for Cosmology and Particle Astrophysics, University of Oxford, Keble Road, Oxford OX1 3RH, UK*

Accepted 2020 March 19. Received 2020 March 3; in original form 2019 August 6

ABSTRACT

The cross-correlation of gravitational wave strain with upcoming galaxy surveys probes theories of gravity in a new way. This method enables testing the theory of gravity by combining the effects from both gravitational lensing of gravitational waves and the propagation of gravitational waves in space–time. We find that within 10 yr the combination of the Advanced LIGO (Laser Interferometer Gravitational-Wave Observatory) and VIRGO (Virgo interferometer) detector networks with planned galaxy surveys should detect weak gravitational lensing of gravitational waves in the low-redshift Universe ($z < 0.5$). With the next-generation gravitational wave experiments such as Voyager, LISA (Laser Interferometer Space Antenna), Cosmic Explorer, and the Einstein Telescope, we can extend this test of the theory of gravity to larger redshifts by exploiting the synergies between electromagnetic wave and gravitational wave probes.

Key words: gravitational lensing; weak – gravitational waves – large-scale structure of Universe.

1 INTRODUCTION

The lambda cold dark matter (ΛCDM) model of cosmology matches well all of the best available data sets probing cosmic microwave background (CMB), galaxy distributions, and supernovae (Alam et al. 2017; Abbott et al. 2018, 2019; Aghanim et al. 2018; Jones et al. 2019). However, 95 per cent of the content of this model is composed of dark energy and dark matter that is not yet understood. Several theoretical models aid our understanding of this unknown part of the Universe and lead to observable predictions that can be explored using electromagnetic probes of the Universe. With the discovery of gravitational waves (Abbott et al. 2016a, 2017b), a new observational probe has opened up that is capable of bringing new insights into our studies of the Universe. Study of the imprints of the dark matter and late-time cosmic acceleration on gravitational waves will provide new avenues for understanding these unknowns.

With the ongoing ground-based gravitational wave observatories such as Advanced LIGO (Laser Interferometer Gravitational-Wave Observatory; Abbott et al. 2016c) and VIRGO (Virgo interferometer; Acernese et al. 2015), and with the upcoming observatories such as KAGRA (Large-Scale Cryogenic Gravitational Wave Telescope; Akutsu et al. 2019) and LIGO-India (Unnikrishnan 2013), we can

measure the gravitational wave signals from binary neutron stars (NS–NSs), stellar mass binary black holes (BH–BHs), and BH–NS systems over the frequency range 10–1000 Hz and up to a redshift of about 1. Along with the ground-based gravitational wave detectors, space-based gravitational wave experiments such as LISA (Laser Interferometer Space Antenna; Klein et al. 2016; Amaro-Seoane et al. 2017) are going to measure the gravitational wave signals emitted from supermassive BH–BHs in the frequency range $\sim 10^{-4}$ to 10^{-1} Hz. In the future, with ground-based gravitational wave experiments such as Voyager, Cosmic Explorer (Abbott et al. 2017a), and the Einstein Telescope,¹ we will be able to probe gravitational wave sources up to redshifts of $z = 8$ and $z = 100$ (Sathyaprakash et al. 2019). This exquisite multifrequency probe of the Universe is going to provide an avenue towards understanding the history of the Universe up to high redshifts and unveil the true nature of dark energy and dark matter.

In this paper, we explore the imprints of the cosmic density field on astrophysical gravitational waves and forecasts for measuring them using cross-correlations with the galaxy density field and galaxy weak lensing. Intervening cosmic structures induce distortions, namely magnifications and demagnifications in the gravitational wave signal when gravitational waves propagate through

* E-mail: mukherje@iap.fr

¹<http://www.et-gw.eu>

space–time. According to the theory of general relativity, these distortions should be universal for gravitational wave signals of any frequency for a fixed density field. These imprints should exhibit correlations with other probes of the cosmic density field such as galaxy surveys, as both of the distortions have a common source of origin.

We estimate the feasibility of measuring the lensing of the gravitational wave signals emitted from astrophysical sources in the frequency bands 10–1000 and 10^{-4} to 10^{-1} Hz by cross-correlating with the upcoming large-scale structure surveys such as DESI (Dark Energy Spectroscopic Instrument; Aghamousa et al. 2016), EUCLID (Refregier et al. 2010), LSST (Large Synoptic Survey Telescope; LSST Science Collaboration 2009), SPHEREx (Dore et al. 2018a), and WFIRST (Wide Field Infrared Survey Telescope; Dore et al. 2018b), which also probe the cosmic density field. The cross-correlation of the gravitational wave signal with the cosmic density field is going to validate the theory of gravity, nature of dark energy, and the impact of dark matter on gravitational wave with a high Signal to Noise Ratio (SNR) over a large range of redshift as discussed in Section 5. The autocorrelation of the gravitational wave sources can also be used as a probe of the lensing signal. However, this is going to be important in the regime of large numbers of gravitational wave sources with high statistical significance such as from the Einstein Telescope² and Cosmic Explorer (Abbott et al. 2017a).

The paper is organized as follows. In Section 2, we discuss the effect of lensing on the galaxy distribution and on gravitational waves. In Section 3, we discuss the implication of the gravitational lensing of gravitational waves in validating the theory of gravity and the standard model of cosmology. In Sections 4 and 5, we obtain the estimator for measuring the signal and the forecast of measuring this from the upcoming gravitational wave observatories and Large Scale Structure (LSS) missions. Finally, in Section 6, we discuss the conclusions of this work and its future scope.

2 WEAK LENSING

The general theory of relativity predicts universal null geodesics for both gravitational wave and electromagnetic wave, which can be written in terms of the Friedmann–Lemaître–Robertson–Walker (FLRW) metric with line elements given by $ds^2 = -dt^2 + a(t)^2(dx^2 + dy^2 + dz^2)$, where $a(t)$ is the scale factor, which is set to 1 at present and decreases to zero in the past. However, in the presence of density fluctuations, both electromagnetic and gravitational waves propagate along the perturbed FLRW metric that can be written as $ds^2 = -(1 + 2\Phi)dt^2 + a(t)^2(1 + 2\Psi)(dx^2 + dy^2 + dz^2)$. One of the inevitable effects of matter perturbations on both electromagnetic and gravitational waves is gravitational lensing that can lead to magnification, spatial deflections, and time delays in the arrival times of the signal (Kaiser & Squires 1993; Kaiser 1998; Bartelmann & Schneider 2001). In this paper, we discuss the aspect of gravitational weak lensing due to the distribution of the density fluctuations in the Universe and its effect on cosmological observables such as the galaxy field and gravitational waves.

2.1 Weak lensing of galaxies

The observed distribution of the galaxies can be translated into a density field as a function of sky position and redshift of the

source as

$$\delta(\hat{n}, z) = \frac{\rho_m(\hat{n}, z)}{\bar{\rho}_m(z)} - 1, \quad (1)$$

where $\rho_m(\hat{n}, z)$ is the matter density at a position \hat{n} at the redshift z and $\bar{\rho}_m$ denotes the mean density at z . The density field of the galaxies is assumed to be a biased tracer of the underlying dark matter density field that can be written in Fourier space in terms of the scale-dependent bias $b_g(k)$ as $\delta_g(k) = b_g(k)\delta_{DM}(k)$. In the Fourier domain, we define the galaxy power spectrum in terms of the dark matter power spectrum by the relation $P_g(k) = b_g(k)^2 P_{DM}(k)$, where the power spectrum is defined as $\langle \delta_{X'}(k)\delta_X^*(k') \rangle = (2\pi)^3 P_{X'X}(k)\delta_D(\vec{k} - \vec{k}')$ (δ_D denotes the Dirac delta function).

The inhomogeneous distribution of matter between galaxies and the observer causes distortions in galaxy shapes. The lensing convergence field can be written in terms of the projected line-of-sight matter density as

$$\kappa_g(\hat{n}) = \int_0^{z_s} dz \frac{3}{2} \frac{\Omega_m H_0^2 (1+z)\chi(z)}{cH(z)} \times \int_z^\infty dz' \frac{dn_{gal}(z')}{dz'} \frac{(\chi(z') - \chi(z))}{(\chi(z'))} \delta(\chi(z)\hat{n}, z), \quad (2)$$

where z_s is the redshift of the source plane and $dn_{gal}(z')/dz'$ is the normalized redshift distribution of galaxies. The convergence field is related to the cosmic shear by the relation (Kaiser 1998)

$$\kappa_g(\vec{k}) = \frac{k_1^2 - k_2^2}{k_1^2 + k_2^2} \gamma_1(\vec{k}) + \frac{k_1 k_2}{k_1^2 + k_2^2} \gamma_2(\vec{k}), \quad (3)$$

where γ_1 and γ_2 are the cosmic shears in the Fourier space with $\vec{k} = (k_1, k_2)$. From the observables such as the galaxy distributions and its shape, the lensing field can be inferred from the data of the upcoming galaxy surveys (LSST Science Collaboration 2009; Refregier et al. 2010; Aghamousa et al. 2016; Dore et al. 2018a, b).

2.2 Weak lensing of gravitational wave

The strain of the gravitational waves from coalescing binaries can be written in terms of the redshifted chirp mass $\mathcal{M}_z = (1+z)\mathcal{M}$ as (Hawking & Israel 1987; Cutler & Flanagan 1994; Poisson & Will 1995; Maggiore 2008)

$$h(f_z) = \mathcal{Q}(\text{angles}) \sqrt{\frac{5}{24}} \frac{G^{5/6} \mathcal{M}_z^2 (f_z \mathcal{M}_z)^{-7/6}}{c^{3/2} \pi^{2/3} d_L} e^{i\phi_z}, \quad (4)$$

where $\mathcal{M} = (m_1 m_2)^{3/5} / (m_1 + m_2)^{1/5}$ is the true chirp mass in terms of the masses of the individual binaries m_1 and m_2 , and d_L is the luminosity distance to the binaries that can be written for the standard Λ CDM model of cosmology as $d_L = (c(1+z)/H_0) \int_0^z dz' / \sqrt{\Omega_m(1+z')^3 + (1-\Omega_m)}$. G and c are the gravitational constant and speed of light, respectively. Propagation of the gravitational wave in the presence of a matter distribution leads to magnification in the strain of gravitational waves in the geometrical optics limit that can be written as³ (Takahashi 2006; Cutler & Holz 2009; Laguna et al. 2010; Camera & Nishizawa 2013; Bertacca et al. 2018)

$$\tilde{h}(\hat{n}, f_z) = h(f_z)[1 + \kappa_{gw}(\hat{n})], \quad (5)$$

³The effects of matter perturbations on the gravitational wave signal apart from the effect from lensing are explored in previous studies (Laguna et al. 2010).

²<http://www.et-gw.eu>

where $\kappa_{\text{gw}}(\hat{n})$ is the lensing convergence and can be written in terms of the density fluctuations $\delta(\chi(z)\hat{n}, z)$ along the line of sight by the relation

$$\kappa_{\text{gw}}(\hat{n}) = \int_0^{z_s} dz \frac{3}{2} \frac{\Omega_m H_0^2 (1+z) \chi(z)}{c H(z)} \times \int_z^\infty dz' \frac{dn_{\text{gw}}(z')}{dz'} \frac{(\chi(z') - \chi(z))}{(\chi(z'))} \delta(\chi(z)\hat{n}, z), \quad (6)$$

where $dn_{\text{gw}}(z')/dz'$ is the normalized redshift distribution of the gravitational wave sources. The redshift distribution of the gravitational wave sources can be determined from the electromagnetic counterparts or else can also be estimated by using the clustering of the gravitational wave source positions with the galaxy catalogues (Oguri 2016; Mukherjee & Wandelt 2018). According to the theory of general relativity and the standard model of cosmology, in the absence of anisotropic stress, metric perturbations are related by $\Phi = -\Psi$, and are related to the matter perturbation by the relation

$$\nabla^2 \Phi = 4\pi G a^2 \rho_m \delta, \quad (7)$$

where G is the gravitational constant and ρ_m is the matter density.

3 PROBE OF GENERAL THEORY OF RELATIVITY AND DARK ENERGY

Gravitational waves bring a new window to validate the general theory of relativity and cosmological constant as the correct explanation of the theory of gravity and cosmic acceleration. Propagation of gravitational waves in the presence of cosmic structures brings two avenues to explore the Universe:

(i) The propagation of gravitational wave in the space–time is defined by a perturbed FLRW metric

$$\mathcal{D}_\mu \mathcal{D}^\mu h_{\alpha\beta} + 2R_{\mu\alpha\nu\beta} h^{\mu\nu} = 0, \quad (8)$$

where \mathcal{D}_μ is the covariant derivative and $R_{\mu\alpha\nu\beta}$ is the curvature tensor.

(ii) For a perfect fluid energy–momentum tensor, the evolution of the metric perturbations Φ and Ψ and its relationship with the matter perturbation can be written at all cosmological epochs by the relation (Hu & Sawicki 2007)

$$g(k, z) \equiv \frac{\Psi(k, z) + \Phi(k, z)}{\Psi(k, z) - \Phi(k, z)} = 0, \quad (9)$$

$$\frac{1}{2} \nabla^2 (\Psi(k, z) - \Phi(k, z)) = 4\pi G a^2 \rho_m \delta.$$

Gravitational lensing of gravitational waves is going to probe both of these aspects of the theory of gravity from the observations. Several alternative theories of gravity consider deviations in equation (8) (Cardoso, Dias & Lemos 2003; Saltas et al. 2014; Nishizawa 2018) and equation (9) (Carroll et al. 2006; Bean et al. 2007; Hu & Sawicki 2007; Schmidt 2008; Silvestri, Pogosian & Buniy 2013; Saltas et al. 2014; Baker & Bull 2015; Baker, Psaltis & Skordis 2015; Lombriser & Taylor 2016; Lombriser & Lima 2017; Slosar et al. 2019) such as (i) $g(k, z) \neq 0$; (ii) the modified Poisson equation; (iii) running of the Planck mass that acts like a frictional term leading to damping of the gravitational strain more than the usual damping due to the luminosity distance; (iv) mass of the graviton; (v) speed of propagation of gravitational waves; and (vi) the anisotropic stress term as a source term in the gravitational wave propagation equation (equation 8). A joint analysis of all of these observational aspects can be performed to test the validity of

the general theory of relativity and cosmic acceleration using the framework discussed in this paper.

An avenue to study gravitational wave propagation in the presence of matter perturbations is to cross-correlate the gravitational wave strain with the cosmic density field probed by other avenues such as the galaxy field, CMB, and line-intensity mapping. In this paper, we explore the cross-correlation of the galaxy field with the gravitational wave strain from astrophysical gravitational wave sources that are going to be measured from upcoming gravitational wave observatories such as Advanced LIGO (Abbott et al. 2017a), VIRGO (Acernese et al. 2015), KAGRA (Akutsu et al. 2019), LIGO-India (Unnikrishnan 2013), and LISA (Klein et al. 2016; Amaro-Seoane et al. 2017). The joint study of the gravitational wave data along with the data from large-scale structure and CMB missions will probe all observable signatures (listed above) due to modifications in the theory of gravity and dark energy by measuring the distortion in the gravitational wave strain.

Previous studies have discussed the effect of gravitational lensing of gravitational waves on measuring cosmological parameters using gravitational wave events only (Takahashi 2006; Cutler & Holz 2009; Laguna et al. 2010; Camera & Nishizawa 2013; Bertacca et al. 2018; Congedo & Taylor 2019). The measurement of the luminosity distance using gravitational waves can also probe the curvature of the Universe (Congedo & Taylor 2019). In this work, we examine the cross-correlation of the gravitational wave strain with electromagnetic probes. This approach introduces two new aspects. First, we can study the synergy between the electromagnetic sector and the gravitational wave sector. Different theories of gravity lead to modifications in equations (8) and (9), and a joint estimation of both of these aspects is necessary to constrain these models. Secondly, the cross-correlation study with large samples of data from galaxy surveys makes it possible to detect the lensing signal from noise-dominated gravitational wave data.

4 MEASURING THE LENSING OF THE GRAVITATIONAL WAVE USING CROSS-CORRELATIONS WITH GALAXY SURVEYS

4.1 Theoretical signal

The propagation of the electromagnetic waves and gravitational waves along the same perturbed geodesics brings an inevitable correlation between the galaxy ellipticity and distortion in the gravitational wave strain according to the theory of general relativity and the standard LCDM model of cosmology. The gravitational wave strain gets lensed by the foreground galaxies present between the gravitational wave source and us. The theoretical power spectrum of the gravitational wave lensing in the spherical harmonic basis can be written as⁴

$$C_l^{\kappa_{\text{gw}} \kappa_{\text{gal}}^j} \equiv \langle (\kappa_{\text{gw}})_{lm} (\kappa_{\text{g}})_{l'm'} \rangle \delta_{ll'}^K \delta_{mm'}^K$$

$$= \int \frac{dz}{\chi^2} \frac{H(z)}{c} \left[W_{\kappa_{\text{gw}}}(\chi(z)) W_{\kappa_{\text{g}}}^j(\chi(z)) \times P_\delta((l+1/2)/\chi(z)) (\chi(z)) \right],$$

⁴We have used the Limber approximation ($k = (l+1/2)/\chi(z)$).

$$\begin{aligned}
 C_i^{\kappa_{\text{gw}}\delta^j} &\equiv \langle (\kappa_{\text{gw}})_{lm} \delta_{l'm'} \rangle \delta_{ll'}^K \delta_{mm'}^K \\
 &= \int \frac{dz}{\chi^2} \frac{H(z)}{c} b_g \left[W_{\kappa_{\text{gw}}}(\chi(z)) W_{\delta}^j(\chi(z)) \right. \\
 &\quad \left. \times P_{\delta}((l+1/2)/\chi(z))(\chi(z)) \right], \quad (10)
 \end{aligned}$$

where $W_{\kappa_{\text{gw}}}^i$, $W_{\kappa_g}^i$, and W_{δ}^i are the kernels for gravitational wave lensing, galaxy lensing, and the galaxy field, respectively, for the tomographic bins indicated by the bin index j in redshift, which can be defined as

$$\begin{aligned}
 W_{\kappa_{\text{gw}}/\kappa_{\text{gal}}}(\chi(z)) &= \frac{1}{H(z)} \int_z^{\infty} dz' \frac{dn_{\text{gw}/\text{gal}}(z')}{dz'} \frac{(\chi(z') - \chi(z))}{(\chi(z'))}, \\
 W_{\delta}^j(\chi(z)) &= \frac{dn}{dz}(z_j). \quad (11)
 \end{aligned}$$

In this analysis, we have taken a linear bias model with the value of the bias parameter as $b_g = 1.6$ (Anderson et al. 2012; Alam et al. 2017; Desjacques, Jeong & Schmidt 2018) and the non-linear dark matter power spectrum from the numerical code CLASS (Blas, Lesgourgues & Tram 2011; Lesgourgues 2011). The power spectra for galaxy lensing and gravitational wave lensing, $c_i^{\kappa_{\text{gw}}\delta^j}$ and $c_i^{\kappa_{\text{gal}}\delta^j}$, are plotted in Fig. 1 as a function of the redshift of the gravitational wave sources. The redshift distribution of the gravitational wave sources is taken as $(dn_{\text{gw}}/dz)(z_s) = \delta(z - z_s)$ and the distribution of the galaxies is taken according to

$$\begin{aligned}
 \frac{dN}{dz}(z_s) &= z_s^2 \exp(-(z_s/z_0)^{3/2}) \quad \text{Model-I,} \\
 \frac{dN}{dz}(z_s) &= \left(\frac{z_s/z_0}{2z_0} \right)^2 \exp(-z_s/z_0) \quad \text{Model-II.} \quad (12)
 \end{aligned}$$

The signal of the cross-correlation gets stronger at high redshifts due to more overlap between the gravitational wave lensing kernel and the galaxy kernel.

4.2 Estimator

The observed gravitational wave signal depends upon both gravitational wave strain from the source and the effect from the gravitational wave propagation, which can be expressed according to equation (5). The observed D_L from the gravitational wave strain can be written as

$$\begin{aligned}
 D_L(\hat{n}) &= \frac{d_L(\hat{n})}{1 + \kappa(\hat{n})} + \epsilon_{\text{gw}}(\hat{n}), \\
 &= d_L(\hat{n})(1 - \kappa(\hat{n})) + \epsilon_{\text{gw}}(\hat{n}) + O(\kappa^2), \quad (13)
 \end{aligned}$$

where ϵ_{gw} is the observational error from the gravitational wave observation with zero mean and $d_L = (c(1+z_s)/H_0) \int_0^{z_s} dz' / \sqrt{\Omega_m(1+z')^3 + (1-\Omega_m)}$. In the weak lensing limit $\kappa_{\text{gw}} \ll 1$, which is used to obtain the second equation in equation (13). The luminosity distance can be inferred independently of the chirp mass using the relation derived by Schutz (1986):

$$\begin{aligned}
 D_L \propto \frac{1}{\bar{h}(t)\tau\nu^2}, \quad \text{where} \quad \tau &\equiv \left(\frac{dv/dt}{\nu} \right)^{-1} \propto \frac{\pi M_z^2}{(\pi M_z)^{11/3} \nu^{8/3}} \\
 \text{and} \quad \bar{h}(t) &\propto \frac{M_z(\pi\nu_z M_z)^{2/3}}{d_L}, \quad (14)
 \end{aligned}$$

where τ is the time-scale related to the change of the frequency of the gravitational wave signal and \bar{h} is the gravitational wave

strain averaged over detectors and source orientations. However, the source inclination angle is important to estimate the luminosity distance accurately (Nissanke et al. 2010). By using the two polarization states of the gravitational wave signal h_+ and h_{\times} , the degeneracy between the source inclination angle and luminosity distance can be lifted (Nissanke et al. 2010).

Equation (13) shows that there exists a multiplicative bias to κ_{gw} from d_L . So, in order to remove this bias, we need to make an estimate of the true luminosity distance for each source. The estimate of true luminosity distance to the gravitational wave sources can be estimated using the redshift (z_s) of the source (from the electromagnetic counterparts; Nissanke, Kasliwal & Georgieva 2013) and best-fitting cosmological parameters (obtained using the data from other cosmological probes such as CMB, supernovae, etc.) in the relation $d_L^{\text{es}} = d_L(1 + \epsilon_s)$, where ϵ_s is the error in the measurement of true d_L due to redshift error and the error in best-fitting cosmological parameters. Then, the estimator for κ_{gw} using the ratio of D_L and d_L^{es} is

$$\begin{aligned}
 \hat{D}_L(\hat{n}) &\equiv 1 - \frac{D_L(\hat{n})}{d_L^{\text{es}}(\hat{n})} \\
 &= 1 - \frac{(1 - \kappa_{\text{gw}}(\hat{n})) + (\epsilon_{\text{gw}}/d_L)(\hat{n})}{1 + \epsilon_s(\hat{n})}. \quad (15)
 \end{aligned}$$

For $\epsilon_s \ll 1$, we can write the above equation as

$$\hat{D}_L(\hat{n}) = \kappa_{\text{gw}}(\hat{n}) - \frac{\epsilon_{\text{gw}}}{d_L}(\hat{n}) + \epsilon_s(\hat{n}) - \epsilon_s(\hat{n})\kappa_{\text{gw}}(\hat{n}). \quad (16)$$

This is feasible for the gravitational wave sources with electromagnetic counterparts, the first case we will discuss. For those gravitational wave sources that do not have electromagnetic counterparts, equation (15) is the estimator of the lensing signal, which produces a multiplicative bias in estimation of the lensing potential κ_{gw} . We will return to this case below and discuss how to remove the bias.

4.2.1 Gravitational wave events with electromagnetic counterpart

For the case when $\epsilon_s \ll 1$, the corresponding estimator for gravitational wave lensing and galaxy lensing cross-correlations in real space can be written as⁵

$$\begin{aligned}
 \hat{C}^{\kappa_{\text{gw}}\kappa_g}(\hat{n} \cdot \hat{n}') &= \langle \hat{D}_L(\hat{n}) \kappa_g(\hat{n}') \rangle \\
 &= \langle \kappa_{\text{gw}}(\hat{n}) \kappa_g(\hat{n}') \rangle + \langle \epsilon_s(\hat{n}) \kappa_g(\hat{n}') \rangle \\
 &\quad - \langle \epsilon_s(\hat{n}) \rangle \langle \kappa_{\text{gw}}(\hat{n}) \kappa_g(\hat{n}') \rangle, \\
 \hat{C}^{\kappa_{\text{gw}}\delta}(\hat{n} \cdot \hat{n}') &= \langle \hat{D}_L(\hat{n}) \delta(\hat{n}') \rangle \\
 &= \langle \kappa_{\text{gw}}(\hat{n}) \delta(\hat{n}') \rangle + \langle \epsilon_s(\hat{n}) \delta(\hat{n}') \rangle \\
 &\quad - \langle \epsilon_s(\hat{n}) \rangle \langle \kappa_{\text{gw}}(\hat{n}) \delta(\hat{n}') \rangle. \quad (17)
 \end{aligned}$$

Here, the term ϵ_s is not correlated with the lensing and density field of the galaxy δ_g and κ_{gw} and hence goes to zero on averaging over a large number of sources. As a result, the estimator of the cross-correlation remains unbiased by any error in the luminosity distance measurement for the gravitational wave sources with electromagnetic counterpart.

⁵The quantities with hat denote the estimator of the signal.

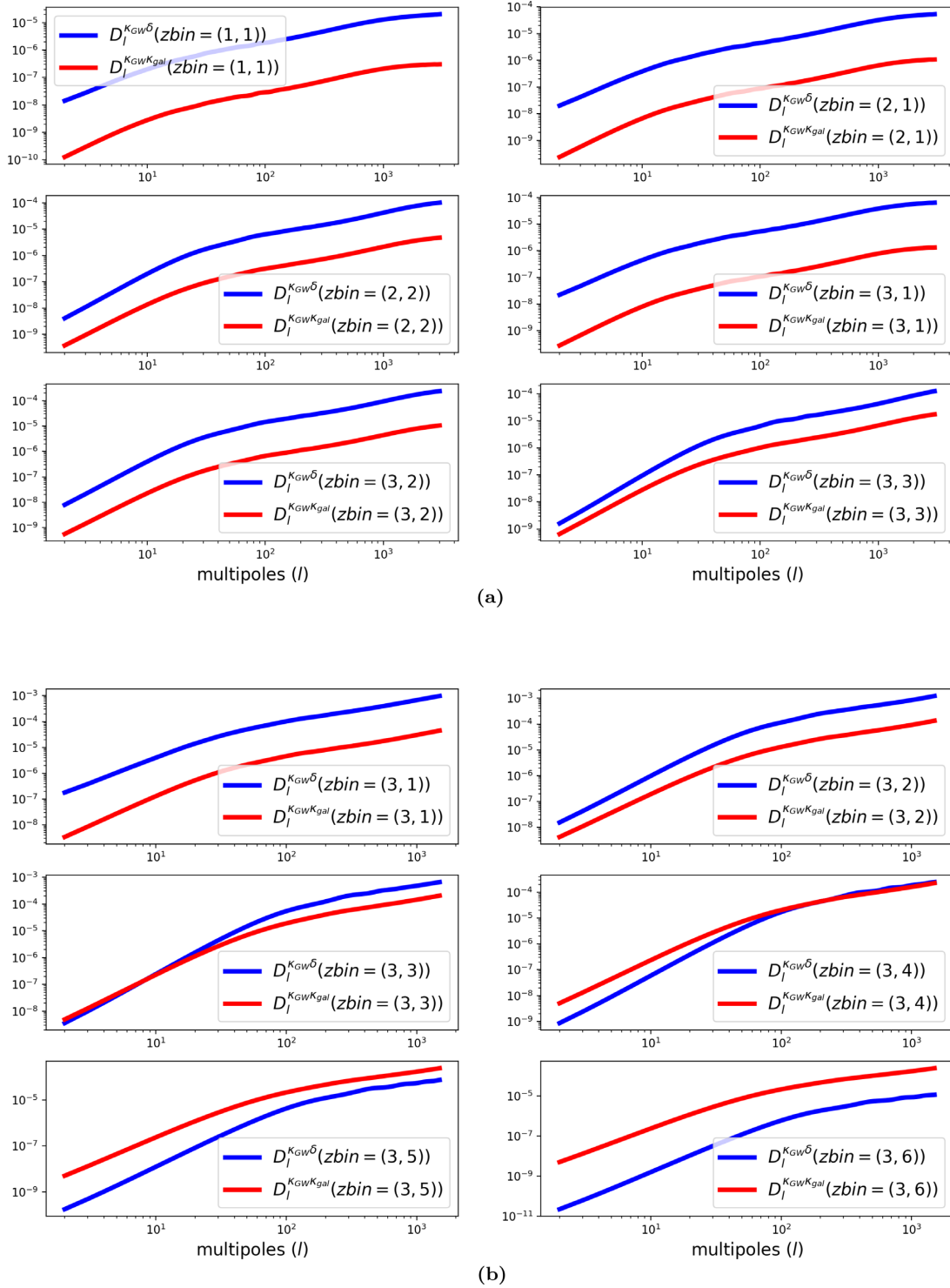


Figure 1. We show the correlation for (a) the LIGO sources and (b) the LISA sources between κ_{gw} with κ_{g} and δ for different tomographic redshift bins indicated by the z_{bin} index given by $(z_{\text{gw}}, z_{\text{g}/\kappa_{\text{g}}})$. The redshift range is taken from $[0, 1]$ and $[0, 3]$ for the LIGO and LISA sources with the bin width $\Delta z = 0.2$ and $\Delta z = 0.5$, respectively. For the galaxy survey, we have taken the redshift distribution for (a) Model-I and (b) Model-II with $z_0 = 0.5$ and for gravitational wave we assume a single source plane $dn_{\text{gw}}/dz(z_s) = \delta_D(z - z_s)$.

4.2.2 Gravitational wave events without electromagnetic counterpart

Returning now to the case of gravitational wave sources without electromagnetic counterparts, the error term $\epsilon_s \sim 1$. The corresponding cross-correlation signal can be written as

$$\begin{aligned}\hat{C}^{\kappa_{\text{gw}}\kappa_{\text{g}}}(\hat{n} \cdot \hat{n}') &= \left\langle \frac{\kappa_{\text{g}}(\hat{n}')\kappa_{\text{gw}}(\hat{n})}{1 + \epsilon_s(\hat{n})} \right\rangle \\ &= C^{\kappa_{\text{g}}\kappa_{\text{gw}}}(\hat{n} \cdot \hat{n}') \left\langle \frac{1}{1 + \epsilon_s(\hat{n})} \right\rangle, \\ \hat{C}^{\kappa_{\text{gw}}\delta}(\hat{n} \cdot \hat{n}') &= \left\langle \frac{\kappa_{\text{gw}}(\hat{n})\delta(\hat{n}')}{1 + \epsilon_s(\hat{n})} \right\rangle \\ &= C^{\kappa_{\text{gw}}\delta}(\hat{n} \cdot \hat{n}') \left\langle \frac{1}{1 + \epsilon_s(\hat{n})} \right\rangle.\end{aligned}\quad (18)$$

The estimated cross-correlation signal can have a multiplicative bias if $\langle \epsilon_s \rangle \neq 0$ for sources without electromagnetic counterparts. However, for a large number of gravitational wave sources, all that is required to remove this bias is $N_{\text{gw}}(z)$, the redshift distribution of the gravitational wave sources. Using the clustering approach, redshifts of the gravitational wave sources can be obtained using the methods described in Menard et al. (2013), Oguri (2016), and Mukherjee & Wandelt (2018).

These estimators in the spherical harmonic basis⁶ can be expressed as $\hat{C}_l^{\kappa_{\text{gw}}\kappa_{\text{g}}} = [1/(2l+1)] \sum_m (\kappa_{\text{gw}})_{lm} (\kappa_{\text{g}})_{lm}$ and $\hat{C}_l^{\kappa_{\text{gw}}\delta} = [1/(2l+1)] \sum_m (\kappa_{\text{gw}})_{lm} \delta_{lm}$. The real space cross-correlation estimator given in equation (17) is related to the spherical harmonic space cross-correlation estimator by the relation

$$\hat{C}_{\mathcal{X}\mathcal{X}'}(\hat{n} \cdot \hat{n}') = \sum_l \left(\frac{2l+1}{4\pi} \right) P_l(\hat{n} \cdot \hat{n}') \hat{C}_l^{\mathcal{X}\mathcal{X}'}, \quad (19)$$

where $P_l(\hat{n} \cdot \hat{n}')$ are the Legendre polynomials.

The variance of the cross-correlation signal can be written in terms of the available overlapping sky fraction of both the missions f_{sky} as

$$\begin{aligned}\left(\sigma_i^{\text{gw}-X} \right)^2 &= \frac{1}{f_{\text{sky}}(2l+1)} \left((C_l^{\kappa_{\text{gw}}\kappa_{\text{gw}}} + N_l^{\mathcal{D}\mathcal{D}}) \right. \\ &\quad \left. \times (C_l^{XX} + N_l^{XX}) + (C_l^{\kappa_{\text{gw}}X})^2 \right),\end{aligned}\quad (20)$$

where $X \in \text{g}, \kappa_{\text{g}}, N_l^{XX} = \sigma_X^2/n_X$ corresponds to the shape noise ($\sigma_{\kappa_{\text{g}}} = 0.3$) and the galaxy shot noise ($\sigma_{\text{g}} = 1$) for $X = \kappa_{\text{g}}$ and g , respectively. n_X denotes the number density of sources per sr. $N_l^{\mathcal{D}\mathcal{D}}$ is the variance related to the estimation of the gravitational wave lensing signal, which can be written as

$$N_l^{\mathcal{D}\mathcal{D}} = \frac{4\pi}{N_{\text{gw}}} \left(\frac{\sigma_{d_l}^2}{d_l^2} + \frac{\sigma_b^2}{d_l^2} \right) e^{l^2 \theta_{\text{min}}^2 / 8 \ln 2}, \quad (21)$$

where N_{gw} is the number of gravitational wave sources, θ_{min} is the sky localization area of the gravitational wave sources, $\sigma_{d_l}^2$ is the error in the luminosity distance due to the detector noise, and σ_b^2 is the error due to the error in the gravitational wave source redshift and uncertain values of cosmological parameters.

The joint estimation of all the effects from the propagation of the gravitational wave signal can be written in a unified framework

by combining the observable from the gravitational wave and the cosmic probes such as the galaxy surveys δ_{g} and κ_{g} as

$$\mathcal{O} = \begin{pmatrix} \hat{D}_{\text{L}} \\ \hat{\delta} \\ \hat{\kappa}_{\text{g}} \end{pmatrix} \quad (22)$$

and the corresponding covariance matrix can be expressed as

$$C \equiv \langle \mathcal{O}\mathcal{O}^\dagger \rangle = \begin{pmatrix} C_l^{D_{\text{L}}D_{\text{L}}} & \mathbf{C}_l^{\kappa_{\text{gw}}\delta} & \mathbf{C}_l^{\kappa_{\text{gw}}\kappa_{\text{g}}} \\ \mathbf{C}_l^{\kappa_{\text{gw}}\delta} & C_l^{\delta\delta} & C_l^{\delta\kappa_{\text{g}}} \\ \mathbf{C}_l^{\kappa_{\text{gw}}\kappa_{\text{g}}} & C_l^{\delta\kappa_{\text{g}}} & C_l^{\kappa_{\text{g}}\kappa_{\text{g}}} \end{pmatrix}.$$

Here, the terms in bold indicate the new cosmological probes that will be available from the cross-correlation of the gravitational wave signal with the galaxy field. The time dependence of the stochastic gravitational wave signal is another probe to study the unresolved sources (Mukherjee & Silk 2020).

5 FORECAST FOR THE MEASUREMENT OF LENSING OF GRAVITATIONAL WAVE

The measurement of the galaxy lensing/gravitational wave lensing and galaxy/gravitational wave lensing can be explored from upcoming missions. The large-scale structure of the Universe will be probed by future missions such as DESI (Aghamousa et al. 2016), EUCLID (Refregier et al. 2010), LSST (LSST Science Collaboration 2009), SPHEREx (Dore et al. 2018a), and WFIRST (Dore et al. 2018b), having a wide sky coverage and access to galaxies up to high redshifts (about $z \sim 3$). For the large-scale structure surveys, we consider the survey set-up with two different normalized redshift distributions according to equation (12) with the values of $z_0 = 0.2$ and $z_0 = 0.5$ (shown in Fig. 2). We have considered two different sets of number density of galaxies as $n_{\text{g}} = 0.5 \text{ arcmin}^{-2}$ for $z_0 = 0.2$ and 45 arcmin^{-2} for $z_0 = 0.5$ in this analysis. The redshift distribution of the large-scale structure surveys overlaps with the redshift distribution of the gravitational wave sources.

For gravitational waves, we have considered the set-up for both ground-based and space-based gravitational wave experiments such as Advanced LIGO and LISA. For the gravitational wave detectors, we have considered the current instrument noise for Advanced LIGO⁷ and LISA as shown in Fig. 3. The LISA noise curves are calculated using the online tool⁸ with the instrument specifications provided in Table 1 (Klein et al. 2016).

The currently ongoing ground-based gravitational wave observatories such as Advanced LIGO (Abbott et al. 2017a) and VIRGO (Acernese et al. 2015), and the future detectors such as KAGRA (Akutsu et al. 2019) and LIGO-India (Unnikrishnan 2013) will be joining these in the coming decade. These experiments will be capable of reaching up to a redshift of $z \sim 1$ and are going to detect the gravitational wave primarily from stellar origin BH–BH mergers, BH–NS mergers, and NS–NS mergers. The exact event rates of these binary mergers are not yet known and are predicted from the current observation of the gravitational wave events (Abbott et al. 2016b, 2017b).

We have taken the number of the sources of gravitational waves as a free parameter for each of these binary species. Among

⁶ Any field $X(\hat{n})$ can be expressed in the spherical harmonics basis as $X(\hat{n}) = \sum_{lm} X_{lm} Y_{lm}(\hat{n})$.

⁷ <https://dcc.ligo.org/cgi-bin/DocDB/ShowDocument?.submit=Identify&docid=T1800044&version=5>

⁸ <http://www.srl.caltech.edu/~shane/sensitivity/MakeCurve.html>

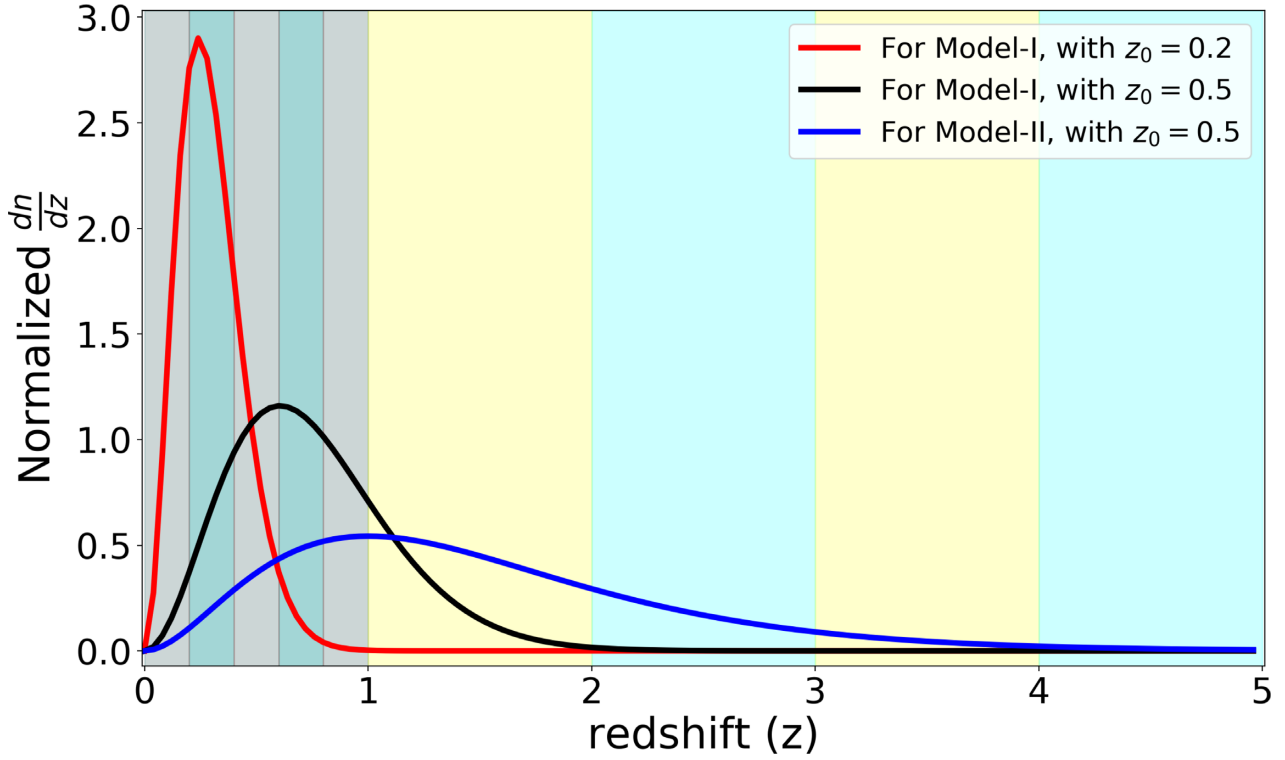


Figure 2. The normalized distribution of the galaxy surveys for Model-I and Model-II given in equation (12). We have used the case with Model-I and $z_0 = 0.2$ for the cross-correlation with the NS–NS and BH–NS sources that can be observed by LIGO. For the BH–BH sources from LIGO, we have used Model-I with $z_0 = 0.5$. For the LISA gravitational wave sources, we have studied the cross-correlation signal for the galaxy distribution shown by Model-II with $z_0 = 0.5$. The coloured bands show the tomographic bins chosen in this analysis with $\Delta z = 0.2$ for LIGO and $\Delta z = 0.5$ for LISA.

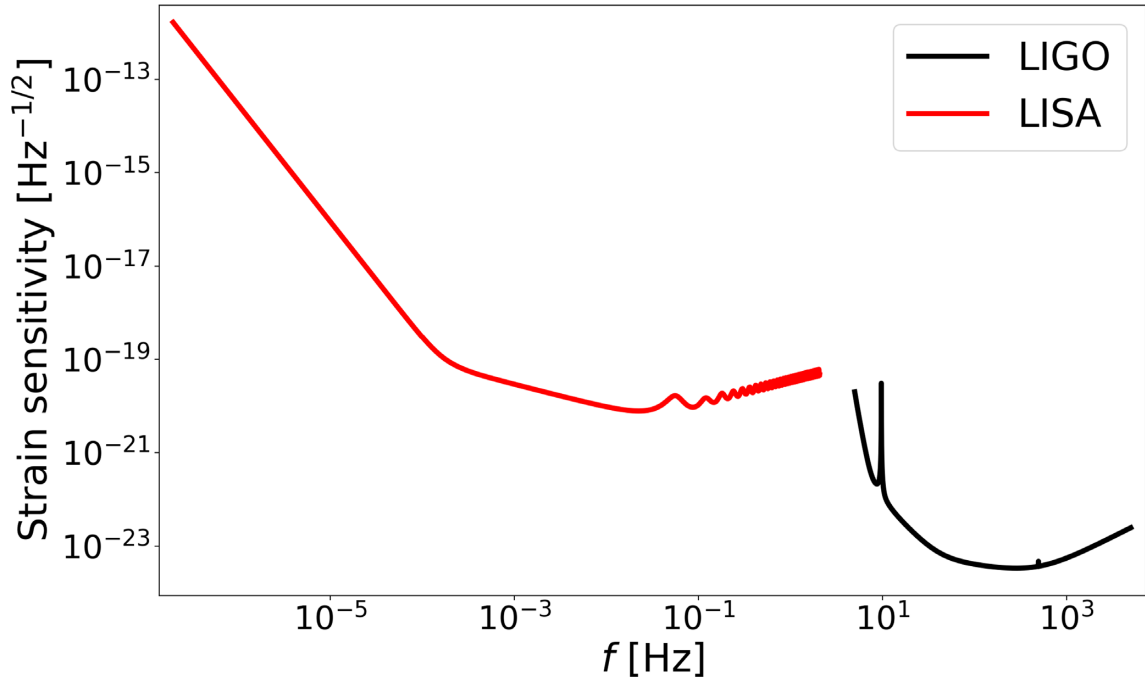


Figure 3. The plot of gravitational wave strain noise for Advanced LIGO and LISA. The Advanced LIGO noise is from the latest projected noise. The LISA noise is plotted for 1 yr of integration time with the LISA instrument specifications given in Table 1.

Table 1. Specifications of LISA instrument properties (Amaro-Seoane et al. 2017) are used with 1 yr of integration time to produce Fig. 3 using the online tool (Larson, Hiscock & Hellings 2000; Larson, Hellings & Hiscock 2002).

Specifications	Values
Arm length	2.5×10^9 m
Optical diameter	0.3 m
Wavelength	1064 nm
Laser power	2.0 W
Optical train efficiency	0.3
Acceleration noise	3×10^{-15} m s ⁻² Hz ^{-1/2}
Position noise	2×10^{-9} m Hz ^{-1/2}
Sensitivity noise floor	Position
Astrophysical noise	White dwarf

these sources, BH–NSs and NS–NSs are expected to have an electromagnetic counterpart (Nissanke et al. 2013; Bhattacharya, Kumar & Smoot 2019) and hence the redshift to these sources can be measured. We have considered the spectroscopic measurement of the source redshift for the electromagnetic counterpart from BH–NS and NS–NS. Sources such as BH–NSs and NS–NSs with electromagnetic counterparts can have an accurate estimation of the sky localization (less than 1 arcsec), which makes it possible to improve the cross-correlation signal with the LSS surveys. For the stellar mass BH–BHs, we do not expect any electromagnetic counterpart, and as a result, the redshift of the source cannot be measured. For BH–BHs, we have considered that the redshift of the source is completely unknown. For BH–BHs without any electromagnetic counterparts, we will be relying only on measurements from the gravitational wave signal, and as a result, the sky localization error is going to have relatively large errors compared to the case of BH–NS and NS–NS. For the combination of five detectors, we can expect about 10 deg² sky localization error in the sources of the gravitational wave (Nissanke et al. 2011; Pankow et al. 2018). In this analysis, we have taken the angular resolution θ (or equivalently the maximum value of l , $l_{\max} \propto 1/\Delta\theta$) as the free parameter and obtained the results for a few different choices.

Along with the ground-based detectors, space-based detectors such as LISA (Klein et al. 2016; Amaro-Seoane et al. 2017; Smith & Caldwell 2019) will also be operational in the next decade and will be able to reach to very high redshifts ($z \sim 20$). These experiments are going to explore supermassive BH–BH systems over a wide range of masses $\sim 10^3$ – $10^7 M_{\odot}$. Such sources are going to be observed in the frequency band 10^{-4} to 10^{-1} Hz for time-scales of days to years before mergers of the binaries. The event rates for these sources are largely unknown and are mainly based on studies made from simulations (Micic et al. 2007). For the heavier supermassive BH–BH systems such as $10^7 M_{\odot}$, the event rates are going to be less than the case for the intermediate supermassive BH–BH systems of mass $10^4 M_{\odot}$, according to our current understanding of the formation of these binaries. We consider three different event rates for unit redshift bins, 50, 100, and 300, in this analysis for LISA. For the supermassive BH–BHs, we can expect to see electromagnetic counterparts over a wide of electromagnetic frequency spectrum (Armitage & Natarajan 2002; Palenzuela, Lehner & Liebling 2010; Giacomazzo et al. 2012; Gold et al. 2014; Farris et al. 2015; Haiman 2018). This is going to be useful for obtaining the redshift of the gravitational wave sources by the electromagnetic follow-up surveys.

In the future, the next-generation gravitational wave observatories will include Voyager,⁹ which is going to achieve an instrument noise of $\sim 10^{-24}$ Hz^{-1/2}. There are also proposals for ground-based observatories with larger baselines such as the Einstein Telescope (Hild et al. 2011) and Cosmic Explorer (Abbott et al. 2017a). These observatories are capable of exploring stellar mass BH–BHs, BH–NSs, and NS–NSs up to a redshift of about $z \sim 20$ for the frequency range 10–1000 Hz. These observatories are going to have orders of magnitude improvement in the instrument noise over LIGO. As a result, our proposed methodology is going to be an exquisite probe of the Universe for better understanding gravity, dark matter, and dark energy by combining the probes from gravitational wave and electromagnetic wave. In future work, we will estimate the prospects of this approach for the next-generation gravitational wave detectors.

The signal-to-noise ratio for the measurement of the cross-correlation of the gravitational wave lensing by cross-correlating with the galaxy lensing ($X = \kappa_{\text{gw}}$) and with the galaxy density field ($X = \delta$) can be estimated using $(S/N)^2 = \sum_l^{\max} C_l^{\kappa_{\text{gw}} X} / (\sigma^{\kappa_{\text{gw}} X})^2$. Using the gravitational wave detector noise, we estimate the error in the luminosity distance σ_{d_l} using a Fisher analysis by considering the two polarization states of the gravitational wave signal:

$$F_{D_l D_l} = \sum_{+, \times} \frac{1}{2} \int_0^{\infty} 4f^2 d \ln f \frac{\partial h_{+, \times}}{\partial D_l} \frac{1}{|h_n(f)|^2} \frac{\partial h_{+, \times}}{\partial D_l}. \quad (23)$$

The corresponding Cramer–Rao bound on the parameters is obtained as $\sigma_{D_l} = \sqrt{(F_{D_l D_l}^{-1})}$. The noise due to lensing causes an error in the estimation of the luminosity distance. This can be written in terms of the fitting form as given by Hirata, Holz & Cutler (2010). The error in the redshift $\sigma_z = C(1+z)$ of the gravitational wave sources leads to an additional error in the estimation of the d_l^{es} as $\sigma_s = (\partial d_l / \partial z) \sigma_z$. We have taken $C = 0.03$ for the cases with photometric measurements of the redshift, and $C = 0$ for spectroscopic measurements of the redshift.

In Figs 4 and 5, we show the cumulative SNR for the measurement of $C_l^{\kappa_{\text{gw}} \kappa_{\text{g}}}$ and $C_l^{\kappa_{\text{gw}} \delta}$ signals for NS–NSs, BH–NS systems, and BH–BHs, respectively. For NS–NSs, current gravitational wave detectors will be able to detect individual objects with high SNR for redshifts $z < 0.2$. As a result, we need to consider galaxy surveys that are going to probe the low-redshift Universe, such as DESI (Aghamousa et al. 2016). Using the galaxy distribution shown by the red colours in Fig. 2, we estimate the cumulative SNR up to redshift $z = 0.2$ for $l_{\max} = 3000$ and assuming spectroscopic measurements of the redshifts of the NS–NSs. Detection is not possible for the currently considered event rate within 5 yr of observation time from $C_l^{\kappa_{\text{gw}} \kappa_{\text{g}}}$. However, for $C_l^{\kappa_{\text{gw}} \delta}$, we can expect a cumulative SNR of three detections of the signal up to redshift $z = 0.2$ for the highest event rates and the best sky fraction scenario. For the redshift range $0.3 > z > 0.2$, LIGO will be detecting several very low SNR gravitational wave events. If the cross-correlation signal with the low-SNR gravitational wave events (which may not be considered as a detected event) and the electromagnetic counterpart of these sources can be identified, then more than a 3σ measurement is possible only from $C_l^{\kappa_{\text{gw}} \delta}$. However, this scenario is extremely rare and the detection of the signal beyond $z > 0.2$ is unlikely.

For the BH–NS systems, we have estimated the SNR for $M_{\text{NS}} = 1.5 M_{\odot}$ and $M_{\text{BH}} = 30 M_{\odot}$. These sources can be identified as individual events for redshifts below 0.5 and we considered the low-

⁹<https://dcc.ligo.org/public/0142/T1700231/003/T1700231-v3.pdf>

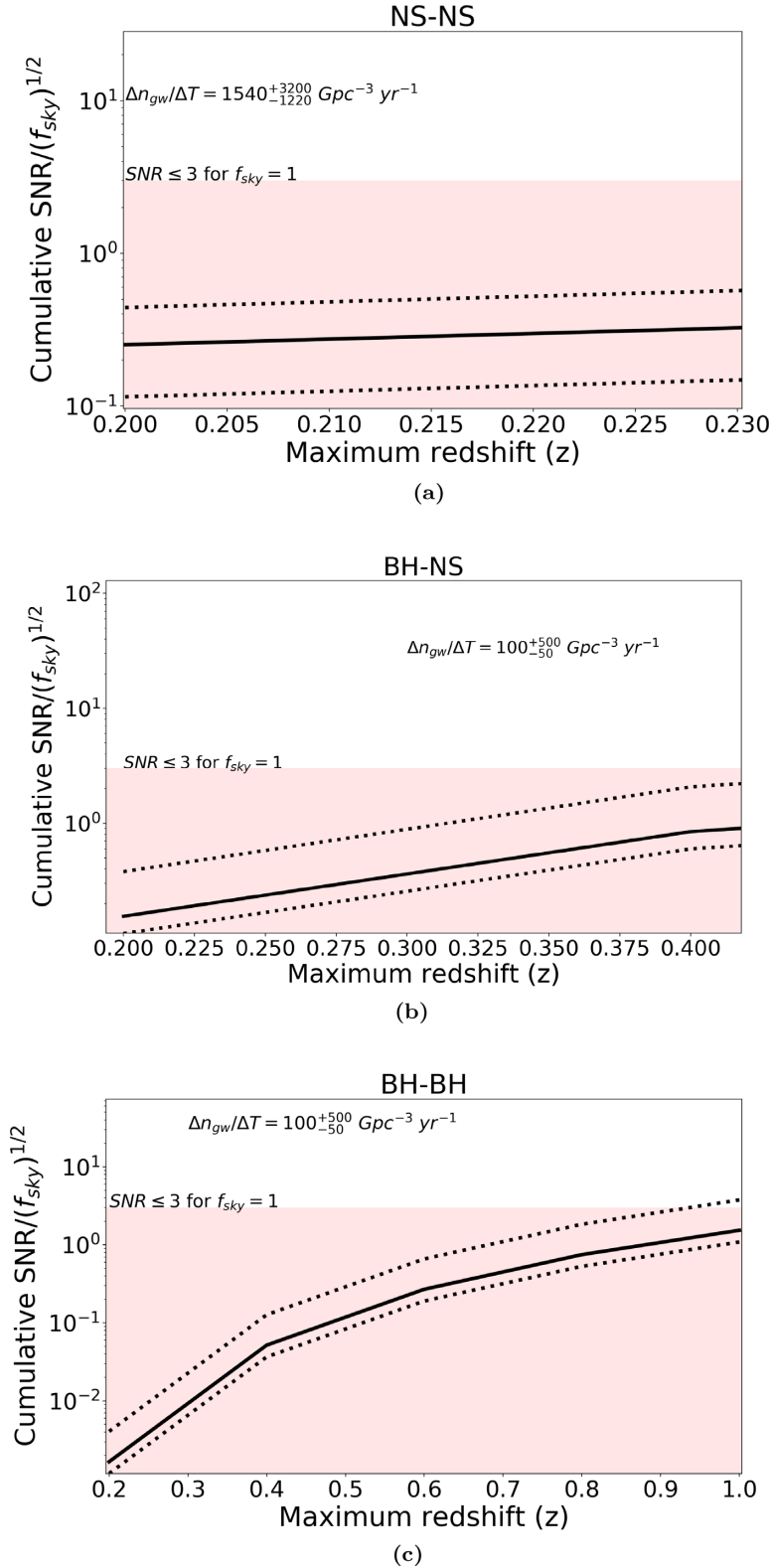


Figure 4. The cumulative SNR for the measurement of the cross-correlation between gravitational wave lensing and galaxy lensing $C_l^{k_{\text{gw}}k_{\text{g}}}$ for an observation time of 5 yr with the instrument noise of Advanced LIGO. (a) For the NS–NS, the detection threshold of the gravitational wave sources above redshift of 0.2 is going to be less than 10σ and hence will not be identified as a LIGO event. (b) For BH–NS, we have considered here the case for a mass ratio of 20 with $M_{\text{total}} = 31.5 M_{\odot}$. (c) The BH–BH sources are considered for equal mass ratios with $M_{\text{total}} = 60 M_{\odot}$. The region shaded in pink indicates below 3σ detection of the cosmological signal. The dotted line indicates the upper and lower limits of the event rates, and the solid line indicates the mean value of the event rates.

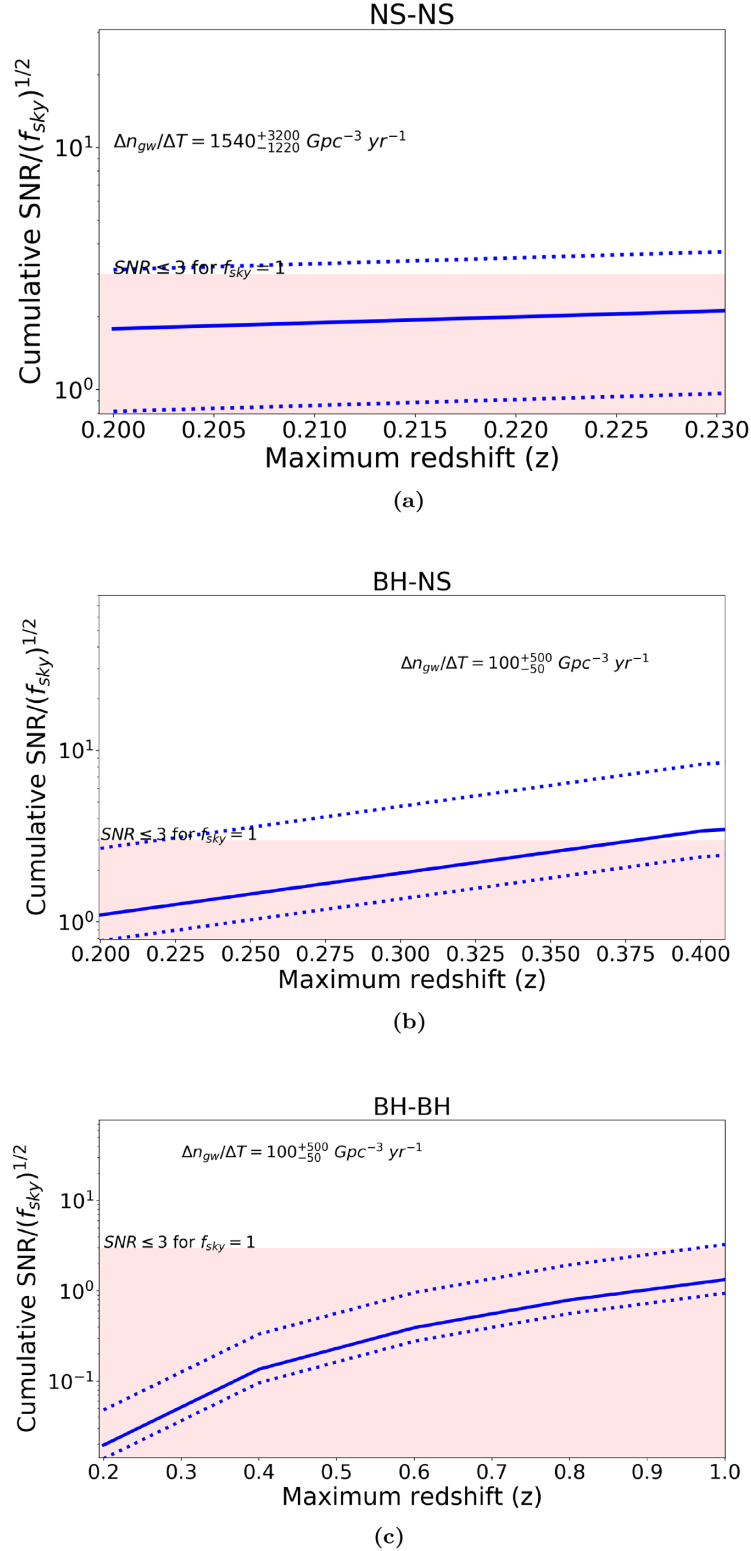


Figure 5. The cumulative SNR for the measurement of the cross-correlation between gravitational wave lensing and galaxy field $C_l^{K_{\text{gw}}\delta}$ for an observation time of 5 yr with the instrument noise of Advanced LIGO. (a) For the NS–NS, the detection threshold of the gravitational wave sources above a redshift of 0.2 is going to be less than 10σ and hence will not be identified as a LIGO event. (b) For BH–NS, we have considered here the case for a mass ratio of 20 with $M_{\text{total}} = 31.5 M_{\odot}$. (c) The BH–BH sources are considered for equal mass ratio with $M_{\text{total}} = 60 M_{\odot}$. The region shaded in pink indicates below 3σ detection of the cosmological signal. The dotted line indicates the upper and lower limits of the event rates, and the solid line indicates the mean value of the event rates.

redshift galaxy survey as shown by the red coloured curve in Fig. 2 to estimate the cross-correlation signal between galaxy lensing and gravitational wave lensing. The measurability of the signal remains weak at nearly all the values of redshift for $C_l^{k_{\text{gw}}k_{\text{g}}}$ with $l_{\text{max}} = 3000$. However, the signal from $C_l^{k_{\text{gw}}\delta}$ can be detected with high SNR for redshift $z > 0.35$ from the sources of the gravitational wave that will be detected by Advanced LIGO-like detectors. BH–NS systems with the lower (or higher) mass of the BH can be identified as individual events only up to a lower (or higher) redshift, and the corresponding detection threshold will vary. The BH–NS systems are the best scenario for studying the cross-correlation signal as this can have an electromagnetic counterpart and can also be detected up to a high redshift than for the NS–NS systems.

For the BH–BH systems, with $M_{\text{total}} = 60 M_{\odot}$, gravitational wave events can be detected up to a redshift $z = 1$. These sources are possibly not going to have electromagnetic counterparts, and as a result, the redshifts of the objects will remain unknown. We have considered the redshift of the gravitational wave sources to be unknown to obtain the forecast for BH–BHs. Along with the absence of the redshifts, these sources are going to have poor sky localization $\sim 10 \text{ deg}^2$ even with the five-detector network (LIGO–H, LIGO–L, VIRGO, KAGRA, LIGO–India; Pankow et al. 2018). Using a minimum sky localization error of 10 deg^2 and for the case with unknown redshift, we estimate the measurability of $C_l^{k_{\text{gw}}k_{\text{g}}}$ and $C_l^{k_{\text{gw}}\delta}$ for a galaxy survey shown by the black curve in Fig. 2 (which reaches up to redshift $z = 1$). The measurability of the signal remains marginal for 5 yr of observation time with the current estimate of the LIGO events. The estimates of the mean signal can also be biased for a lesser number of gravitational wave samples, due to the unavailability of the true luminosity distance to the gravitational wave source (as shown in equation 16). For a large number of the gravitational wave sources, clustering redshift of the gravitational wave source can be inferred by using the spatial correlations (Menard et al. 2013; Oguri 2016; Mukherjee & Wandelt 2018).

Detection of more events is going to improve the projected SNR. In these estimates of the SNR for NS–NSs, BH–NSs, and BH–BHs, we have only considered the inspiral phase of the gravitational wave signal. Further improvement of the SNR is possible if we include merger and the ring-down phase of the gravitational wave strain. This will be considered in a future analysis, including the complete waveform of the gravitational wave signal.

For the space-based gravitational wave detectors such as LISA, the gravitational wave events are going to be detected up to a redshift of about $z \sim 20$ (Amaro-Seoane et al. 2017). This enables us to probe the cosmological signal up to a high redshift by cross-correlating with galaxy surveys that reach up to a high redshift. Using the redshift distribution of galaxies shown by the blue curve in Fig. 2 that mimics the surveys such as LSST, we estimate the SNR for the measurability of $C_l^{k_{\text{gw}}k_{\text{g}}}$ and $C_l^{k_{\text{gw}}\delta}$ for different masses of the BH–BHs ranging from 10^4 to 10^7 . In this analysis, we have considered a maximum time period of 1 yr of inspiral phase before the merger. The merger and the ring-down phase for these sources are not considered in the analysis. For the LISA BH–BH sources, we have considered a photometric error of $\sigma_z/(1+z) = 0.03$ in the determination of the redshift of gravitational wave sources from the electromagnetic counterpart. Measurement of the electromagnetic counterpart is also going to be useful to reduce the sky localization error of the source of the gravitational wave and hence improves the detection of the cross-correlation signal. For two different values of l_{max} , $l_{\text{max}} = 200$ and $l_{\text{max}} = 1000$, we estimate the SNR for the measurement of $C_l^{k_{\text{gw}}k_{\text{g}}}$ and $C_l^{k_{\text{gw}}\delta}$ signals for 4 yr of observation time

and show the corresponding estimates in Figs 6 and 7, respectively. As can be seen from these figures, the discovery space from synergy between LISA and LSST is promising for each mass window of BH–BHs. These SNRs are going to improve with the inclusion of the merger and the ring-down phase of the gravitational wave signal. Further improvement in the SNR is possible with the increase in the LISA observation time to 10 yr, increase in the number of gravitational wave event rates, and also with galaxy surveys that can go up to higher redshifts. By combining all the high-redshift probes such as EUCLID (Refregier et al. 2010), LSST (LSST Science Collaboration 2009), SPHEREx (Dore et al. 2018a), and WFIRST (Dore et al. 2018b), the detectability of the signal is going to improve significantly. At redshifts higher than $z > 3$, the temperature and polarization anisotropies of the CMB are going to be a powerful probe to measure the lensing signal to even higher redshifts as shown by Mukherjee, Wandelt & Silk (2019). Using the cross-correlation between CMB lensing and gravitational wave lensing, we are going to have higher SNR measurements from redshift $z > 3$ than possible from the galaxy surveys with the redshift distributions considered in this analysis (Fig. 2). Complementary information from cross-correlation with intensity mapping of the 21-cm line is another avenue to be explored in future work.

6 CONCLUSIONS

The general theory of relativity provides a unique solution to the propagation of gravitational waves that depends upon the underlying space–time metric. Gravitational waves according to the theory of general relativity are massless and should propagate along null geodesics with the speed of light. As a result, in the framework of the standard model of cosmology, gravitational wave should propagate through the perturbed FLRW metric where the perturbations arise due to the spatial fluctuations in the matter density in every position. As a result of this metric perturbation, the gravitational wave strain is distorted. The polarization state of gravitational waves can also be used to constrain the theory of gravity Fesik et al. (2017).

Study of these distortions in the gravitational wave strain while propagating through the perturbed metric can be a direct observational probe of several aspects of fundamental physics, which include (i) the validation of general relativity from the propagation of gravitational wave signals and from the connection between metric perturbations and matter perturbations; (ii) properties of dark energy and its effect on gravitational waves; (iii) gravitational effects of dark matter on gravitational waves and evolution with cosmic redshift; (iv) testing the equivalence principle from the multifrequency character of the gravitational wave signal; and (v) equivalence between the electromagnetic sector and the gravitational sector over the cosmic time-scale.

The coming decade with ongoing and upcoming gravitational wave observatories makes it possible to study these aspects and opens a new window in observational cosmology. The astrophysical gravitational wave signals that are emitted from compact objects of different types, such as white dwarfs, NSs, and BHs, span a vast range of masses, gravitational wave frequencies, and cosmological redshifts. All of these sources are transients and are going to be frequent. As a result, they can probe the underlying theory of gravity and the statistical properties of the cosmological perturbations present in the Universe multiple times from different sources. As a result, all the above-mentioned aspects of fundamental physics can be studied using transient astrophysical gravitational wave sources.

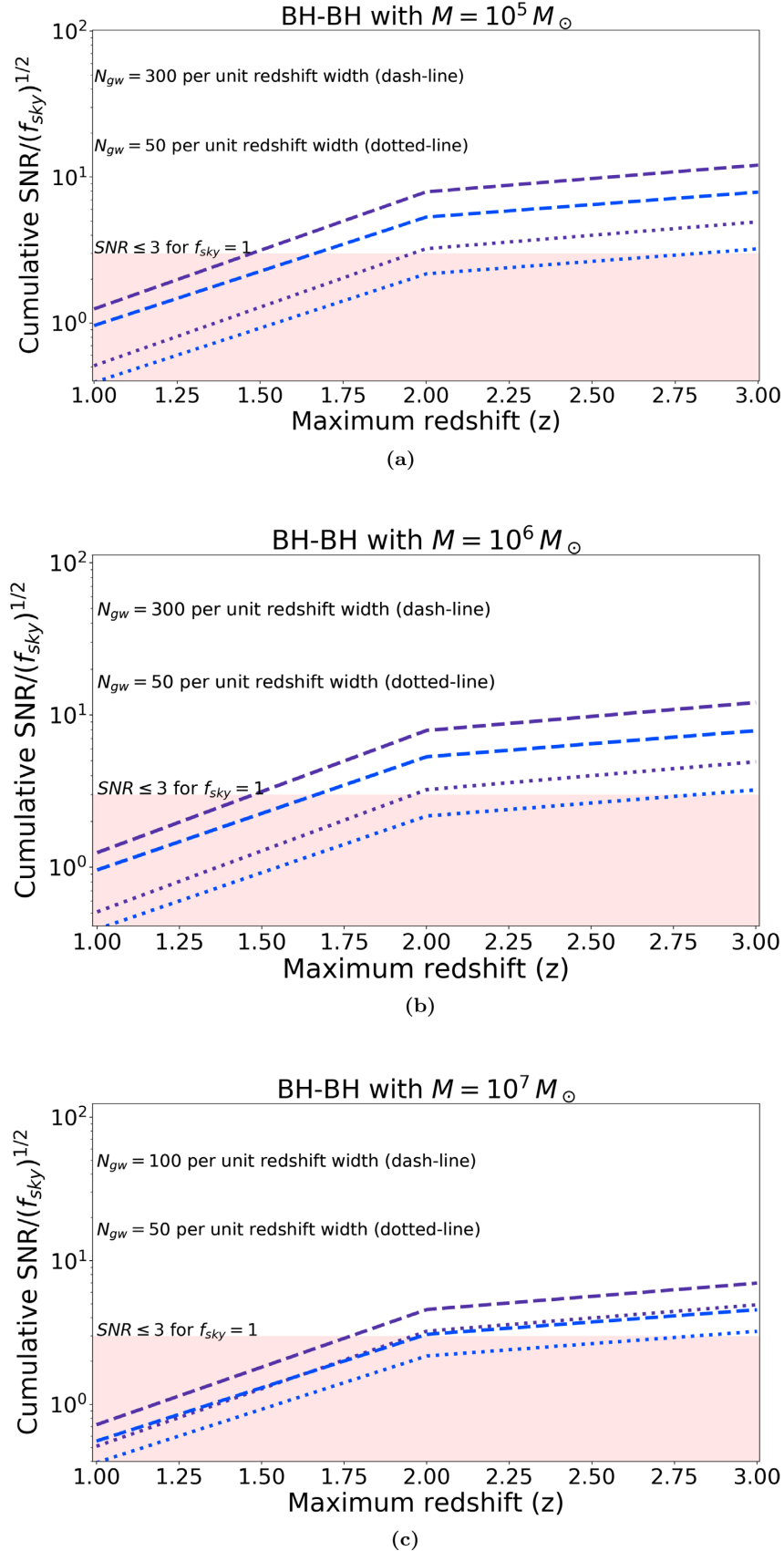


Figure 6. The cumulative SNR for the measurement of the cross-correlation between the gravitational wave lensing and galaxy lensing $C_l^{K_{\text{gw}}K_{\text{g}}}$ from LISA for an observation time of 4 yr for equal mass BH–BHs with individual masses of (a) 10^5 , (b) 10^6 , and (c) 10^7 . The region shaded in pink indicates below 3σ detection of the cosmological signal. The projected SNRs are obtained for two sky localization errors: (i) $\Delta\theta = 1$ deg (shown in blue) and (ii) $\Delta\theta = 0.2$ deg (shown in purple).

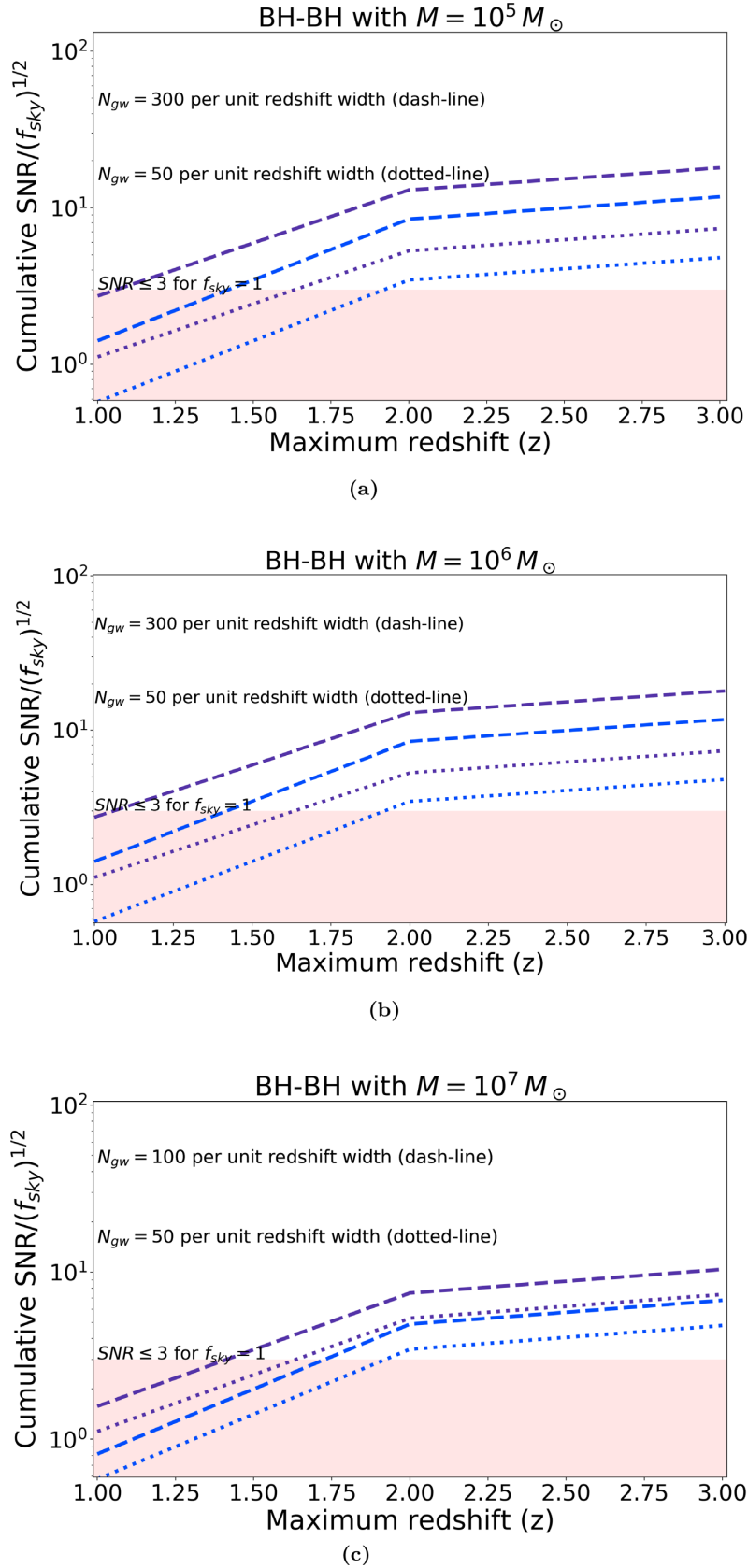


Figure 7. The cumulative SNR for the measurement of the cross-correlation between the gravitational wave lensing and galaxy field $C_l^{k_{\text{gw}}\delta}$ from LISA for an observation time of 4 yr for equal mass BH–BHs with individual masses of (a) 10^5 , (b) 10^6 , and (c) 10^7 . The region shaded in pink indicates below 3σ detection of the cosmological signal. The projected SNRs are obtained for two sky localization errors: (i) $\Delta\theta = 1$ deg (shown in blue) and (ii) $\Delta\theta = 0.2$ deg (shown in purple).

In this paper, we have explored one of the important effects of matter perturbations, the weak lensing of the gravitational wave strain, and propose an avenue to explore this signal using cross-correlations with other cosmological probes such as galaxy surveys. The measurement of the lensing signal leads to a measurement of the evolution of the gravitational potential over a wide range of cosmic redshifts and also probes the connection of the matter perturbation with the gravitational potential. The joint study of cosmic density field and gravitational wave propagation in space–time promises to be a powerful avenue towards a better understanding of the theory of gravity and the dark sector (dark matter and dark energy) of the Universe.

Several alternative theories of gravity and models of dark energy can be distinguished from the evolution of the cosmic structures (Carroll et al. 2006; Bean et al. 2007; Hu & Sawicki 2007; Schmidt 2008; Silvestri et al. 2013; Baker & Bull 2015; Baker et al. 2015; Slosar et al. 2019) and also from the propagation of gravitational wave in space–time (Cardoso et al. 2003; Saltas et al. 2014; Nishizawa 2018). As a result, the studies of the cross-correlations between the gravitational wave signal and cosmic structures should result in a more comprehensive understanding of the theory of gravity and dark energy. The imprint of the lensing potential is also a direct probe of the dark matter distribution in the Universe, and measurement of this via gravitational wave is going to explore the gravitational effects of dark matter on gravitational waves. The measurement of the gravitational lensing signal from gravitational waves with a frequency ranging from 10^{-4} to 10^3 Hz will probe the universality of gravity on a wide range of energy scales and lead to a direct probe of the equivalence principle. Finally, this new avenue is also going to illuminate several hitherto unexplored windows that can be studied from the synergies between electromagnetic waves and gravitational waves.

Ground-based gravitational wave detectors such as LIGO-US (Abbott et al. 2017a), VIRGO (Acernese et al. 2015), KAGRA (Akutsu et al. 2019), and LIGO-India (Unnikrishnan 2013), and space-based gravitational wave detector such as LISA (Klein et al. 2016; Amaro-Seoane et al. 2017) are going to probe a large range of cosmic redshift $0 < z \lesssim 20$ with gravitational wave sources such as NS–NS, BH–NS, stellar mass BH–BH, and supermassive BH–BH. By cross-correlating with the data from upcoming galaxy surveys such as DESI (Aghamousa et al. 2016), EUCLID (Refregier et al. 2010), LSST (LSST Science Collaboration 2009), SPHEREx (Dore et al. 2018a), and WFIRST (Dore et al. 2018b), we will be able to obtain a high SNR detection of the weak lensing signal with these surveys, as shown in Figs 4–7. The measurability is best for the sources with electromagnetic counterparts such NS–NS, BH–NS, and supermassive BH–BHs. For stellar mass BH–BHs, we do not expect electromagnetic counterparts, and hence poorly determined source redshifts. As a result, the measurability of the weak lensing signal is going to be marginal from stellar mass BH–BHs.

We find that the most promising avenue with Advanced LIGO will be the cross-correlation of lensed BH–NS mergers and the galaxy overdensity $C_l^{k_{\text{gw}}\delta}$. The contributions from NS–NSs and BH–BHs are marginal and only improve if the event rates are larger than those considered in this analysis. However, with future surveys such as Cosmic Explorer and the Einstein Telescope, we can explore the spatial cross-correlation of BH–BHs and galaxies in order to obtain the clustering redshift (Menard et al. 2013) of the sources (Oguri 2016). This can result in an improvement in the correlation signal. By fitting the shape of the correlation function between the spatial position of BH–BHs and underlying galaxies, an accurate estimate of the source redshift is possible (Mukherjee & Wandelt 2018)

for a large sample of BH–BHs. The gravitational wave sources from LISA are going to provide a high SNR measurement from both $C_l^{k_{\text{gw}}k_{\text{g}}}$ and $C_l^{k_{\text{gw}}\delta}$ over a vast range of gravitational wave source masses 10^4 – $10^7 M_{\odot}$ by cross-correlating with the large-scale structure surveys with the access to high cosmological redshift. In future work, we will present a joint Bayesian framework for the combined analysis of the gravitational wave data and cosmological data. For this, we use the full gravitational wave waveforms including the inspiral, merger, and ring-down phases, instead of only the inspiral phase considered in this analysis. Inclusion of the merger and ring-down phases is going to improve the SNR presented in this paper.

In summary, we point out a new window for the emerging paradigm of multimessenger observational cosmology with transient sources. This window will exploit both gravitational wave and electromagnetic waves in order to test the propagation and lensing of gravitational waves, potentially leading to high-precision tests of gravity on cosmological scales. In addition to testing gravity in new ways, we expect this probe to be useful for developing an improved understanding of the standard model of cosmology. All the electromagnetic observational probes of the Universe point to additional matter content beyond baryonic matter, entirely inferred through its gravitational effects. The cause of these effects is associated in the standard model of cosmology with a CDM component, which is neither understood theoretically nor directly detected in particle physics experiments. We show in this paper that gravitational waves will bring a new and independent window to confirm the existence of dark matter in the Universe and exploit the gravitational effect of dark matter on gravitational waves as a new and complementary probe on its physical nature. The detailed potential for constraints on the theoretical models from this new observational window, enabled by advances in gravitational wave detector capabilities and a new generation of galaxy redshift surveys, remains to be determined.

ACKNOWLEDGEMENTS

SM would like to thank Karim Benabed, Luc Blanchet, Sukanta Bose, Neal Dalal, Guillaume Faye, Zoltan Haiman, David Spergel, and Samaya Nissanke for useful discussions. The results of this analysis were obtained using the Horizon cluster hosted by Institut d’Astrophysique de Paris. We thank Stephane Rouberol for smoothly running the Horizon cluster. The Flatiron Institute was supported by the Simons Foundation. The work of SM and BDW was also supported by the Labex ILP (reference ANR-10-LABX-63) part of the Idex SUPER, and received financial state aid managed by the Agence Nationale de la Recherche, as part of the programme Investissements d’avenir under the reference ANR-11-IDEX-0004-02. The work of BDW was also supported by the grant ANR-16-CE23-0002. BDW thanks the CCPP at NYU for hospitality during the completion of this work. In this analysis, we have used the following packages: IPYTHON (Pérez & Granger 2007), MATPLOTLIB (Hunter 2007), NUMPY (van der Walt, Colbert & Varoquaux 2011), and SCIPY (Virtanen et al. 2020).

REFERENCES

- Abbott B. P. et al., 2016a, *Phys. Rev. Lett.*, 116, 061102
- Abbott B. P. et al., 2016b, *ApJ*, 833, L1
- Abbott B. P. et al., 2016c, *Phys. Rev. D*, 93, 112004
- Abbott B. P. et al., 2017a, *Class. Quantum Gravity*, 34, 044001
- Abbott B. P. et al., 2017b, *Phys. Rev. Lett.*, 119, 161101
- Abbott T. M. C. et al., 2018, *Phys. Rev. D*, 98, 043526

- Abbott T. M. C. et al., 2019, *ApJ*, 872, L30
- Acernese F. et al., 2015, *Class. Quantum Gravity*, 32, 024001
- Aghamousa A. et al., 2016, preprint (arXiv:1611.00036)
- Aghanim N. et al., 2018, preprint (arXiv:1807.06209)
- Akutsu T. et al., 2019, *Nat. Astron.*, 3, 35
- Alam S. et al., 2017, *MNRAS*, 470, 2617
- Amaro-Seoane P. et al., 2017, preprint (arXiv:1702.00786)
- Anderson L. et al., 2012, *MNRAS*, 427, 3435
- Armitage P. J., Natarajan P., 2002, *ApJ*, 567, L9
- Baker T., Bull P., 2015, *ApJ*, 811, 116
- Baker T., Psaltis D., Skordis C., 2015, *ApJ*, 802, 63
- Bartelmann M., Schneider P., 2001, *Phys. Rep.*, 340, 291
- Bean R., Bernat D., Pogosian L., Silvestri A., Trodden M., 2007, *Phys. Rev. D*, 75, 064020
- Bertacca D., Raccanelli A., Bartolo N., Matarrese S., 2018, *Phys. Dark Univ.*, 20, 32
- Bhattacharya M., Kumar P., Smoot G., 2019, *MNRAS*, 486, 5289
- Blas D., Lesgourgues J., Tram T., 2011, *J. Cosmol. Astropart. Phys.*, 7, 034
- Camera S., Nishizawa A., 2013, *Phys. Rev. Lett.*, 110, 151103
- Cardoso V., Dias O. J. C., Lemos J. P. S., 2003, *Phys. Rev. D*, 67, 064026
- Carroll S. M., Sawicki I., Silvestri A., Trodden M., 2006, *New J. Phys.*, 8, 323
- Congedo G., Taylor A., 2019, *Phys. Rev. D*, 99, 083526
- Cutler C., Flanagan E. E., 1994, *Phys. Rev. D*, 49, 2658
- Cutler C., Holz D. E., 2009, *Phys. Rev. D*, 80, 104009
- Desjacques V., Jeong D., Schmidt F., 2018, *Phys. Rep.*, 733, 1
- Dore O. et al., 2018a, preprint (arXiv:1805.05489)
- Dore O. et al., 2018b, preprint (arXiv:1804.03628)
- Farris B. D., Duffell P., MacFadyen A. I., Haiman Z., 2015, *MNRAS*, 447, L80
- Fesik L. E., Baryshev Y. V., Sokolov V. V., Paturel G., 2017, preprint (arXiv:1702.03440)
- Giacomazzo B., Baker J. G., Miller M. C., Reynolds C. S., van Meter J. R., 2012, *ApJ*, 752, L15
- Gold R., Paschalidis V., Ruiz M., Shapiro S. L., Etienne Z. B., Pfeiffer H. P., 2014, *Phys. Rev. D*, 90, 104030
- Haiman Z., 2018, *Found. Phys.*, 48, 1430
- Hawking S. W., Israel W., 1987, *Three Hundred Years of Gravitation*. Cambridge Univ. Press, Cambridge
- Hild S. et al., 2011, *Class. Quantum Gravity*, 28, 094013
- Hirata C. M., Holz D. E., Cutler C., 2010, *Phys. Rev. D*, 81, 124046
- Hu W., Sawicki I., 2007, *Phys. Rev. D*, 76, 104043
- Hunter J. D., 2007, *Comput. Sci. Eng.*, 9, 90
- Jones D. O. et al., 2019, *ApJ*, 881, 19
- Kaiser N., 1998, *ApJ*, 498, 26
- Kaiser N., Squires G., 1993, *ApJ*, 404, 441
- Klein A. et al., 2016, *Phys. Rev. D*, 93, 024003
- Laguna P., Larson S. L., Spergel D., Yunes N., 2010, *ApJ*, 715, L12
- Larson S. L., Hiscock W. A., Hellings R. W., 2000, *Phys. Rev. D*, 62, 062001
- Larson S. L., Hellings R. W., Hiscock W. A., 2002, *Phys. Rev. D*, 66, 062001
- Lesgourgues J., 2011, preprint (arXiv:1104.2932)
- Lombriser L., Lima N. A., 2017, *Phys. Lett. B*, 765, 382
- Lombriser L., Taylor A., 2016, *J. Cosmol. Astropart. Phys.*, 1603, 031
- LSST Science Collaboration, 2009, preprint (arXiv:0912.0201)
- Maggiore M., 2008, *Gravitational Waves: Volume 1: Theory and Experiments*. Gravitational Waves. Oxford Univ. Press, Oxford
- Menard B., Scranton R., Schmidt S., Morrison C., Jeong D., Budavari T., Rahman M., 2013, preprint (arXiv:1303.4722)
- Micic M., Holley-Bockelmann K., Sigurdsson S., Abel T., 2007, *MNRAS*, 380, 1533
- Mukherjee S., Silk J., 2020, *MNRAS*, 491, 4690
- Mukherjee S., Wandelt B. D., 2018, preprint (arXiv:1808.06615)
- Mukherjee S., Wandelt B. D., Silk J., 2019, preprint (arXiv:1908.08950)
- Nishizawa A., 2018, *Phys. Rev. D*, 97, 104037
- Nissanke S., Holz D. E., Hughes S. A., Dalal N., Sievers J. L., 2010, *ApJ*, 725, 496
- Nissanke S., Sievers J., Dalal N., Holz D., 2011, *ApJ*, 739, 99
- Nissanke S., Kasliwal M., Georgieva A., 2013, *ApJ*, 767, 124
- Oguri M., 2016, *Phys. Rev. D*, 93, 083511
- Palenzuela C., Lehner L., Liebling S. L., 2010, *Science*, 329, 927
- Pankow C., Chase E. A., Coughlin S., Zevin M., Kalogera V., 2018, *ApJ*, 854, L25
- Pérez F., Granger B. E., 2007, *Comput. Sci. Eng.*, 9, 21
- Poisson E., Will C. M., 1995, *Phys. Rev. D*, 52, 848
- Refregier A., Amara A., Kitching T. D., Rassat A., Scaramella R., Weller J., 2010, preprint (arXiv:1001.0061)
- Saltas I. D., Sawicki I., Amendola L., Kunz M., 2014, *Phys. Rev. Lett.*, 113, 191101
- Sathyaprakash B. S. et al., 2019, preprint (arXiv:1903.09260)
- Schmidt F., 2008, *Phys. Rev. D*, 78, 043002
- Schutz B. F., 1986, *Nature*, 323, 310
- Silvestri A., Pogosian L., Buniy R. V., 2013, *Phys. Rev. D*, 87, 104015
- Slosar A. et al., 2019, *Bull. Am. Astron. Soc.*, 51, 97
- Smith T. L., Caldwell R., 2019, *Phys. Rev. D*, 100, 104055
- Takahashi R., 2006, *ApJ*, 644, 80
- Unnikrishnan C. S., 2013, *Int. J. Mod. Phys. D*, 22, 1341010
- van der Walt S., Colbert S. C., Varoquaux G., 2011, *Comput. Sci. Eng.*, 13, 22
- Virtanen P., et al., 2020, *Nature Methods*, 17, 261

This paper has been typeset from a $\text{\TeX}/\text{\LaTeX}$ file prepared by the author.